IEEE Access
Multidisciplinary ⋮ Rapid Review ⋮ Open Access Journal

Received December 26, 2021, accepted January 15, 2022, date of publication January 26, 2022, date of current version February 15, 2022.

Digital Object Identifier 10.1109/ACCESS.2022.3146333

A Multi-Objective Approach for Voltage Stability Enhancement and Loss Reduction Under PQV and P Buses Through Reconfiguration and Distributed Generation Allocation

AKHILESH KUMAR BARNWAL[1], (Graduate Student Member, IEEE), LOKESH KUMAR YADAV[2], AND MITRESH KUMAR VERMA[1], (Member, IEEE)

[1]Indian Institute of Technology (Banaras Hindu University), Varanasi, Uttar Pradesh 221005, India
[2]Department of Electrical Engineering, Rajkiya Engineering College, Ambedkar Nagar, Uttar Pradesh 224122, India

Corresponding author: Akhilesh Kumar Barnwal (akhileshkb.rs.eee16@iitbhu.ac.in)

ABSTRACT This paper proposes a novel approach of voltage stability enhancement and power loss minimization in addition to maintenance of good voltage profile in radial distribution networks through optimally placed distributed generation, network reconfiguration and voltage control of PQV bus through variable reactive power source at P bus. A multi-objective function has been proposed that considers maximum system loadability enhancement and network loss minimization. Optimization of proposed multi-objective function, under distributed generation and network reconfiguration with presence of PQV and P buses in the system have been done using grey wolf optimization technique. Case studies performed on IEEE 33-bus radial distribution system shows that presence of PQV and P buses in the system yields significant enhancement in voltage stability margin under optimal placement of distributed generations and network reconfiguration.

INDEX TERMS Distributed generation, grey wolf optimization, PQV and P buses, reconfiguration.

I. INTRODUCTION

The continuously increasing demand in transmission as well as distribution network has rendered many planning and operational challenges such as maintaining voltage stability, network loss reduction and voltage profile improvement. Voltage stability is the ability of system to maintain bus voltages within permissible limits. According to IEEE/CIGRE joint task force, ''Voltage stability is defined as the ability of a power system to maintain steady voltages at all buses in the system after being subjected to a disturbance from a given initial operating condition'' [1]. The increased load of the distribution network and other disturbances creates risk to voltage instability of the network due to deterioration of voltage profile in significant part of the network. A system with fairly good voltage profile having nearly same voltage magnitude at all the buses at the base case operating point may also face voltage instability under severe contingencies. Thus it is important to maintain sufficient voltage stability margin (the distance between the base case operating point and voltage stability limit). A continuously increasing load increases the chance of voltage collapse within the system. When voltage instability occurs, voltages at some buses may progressively fall or rise that may ultimately lead to voltage collapse. The main factor causing this problem is the inability of the power system to meet the reactive power demand as it is difficult to transmit reactive power under heavily loaded conditions. Voltage stability is a key issue in radial distribution networks as increase in demand may deteriorate voltage at remote buses to unacceptable limits leading to partial/complete blackout [2]. Voltage stability can be examined in terms of maximum loadability (λ_{max}) of the system. Several methods have been reported in literature to evaluate maximum loadability [3]–[6]. Remote end buses of radial distribution networks undergo very low voltages that poses threat of voltage instability as system may reach maximum loadability limit under contingencies [7]. Therefore, proper strategy is required to enhance maximum loadability of these networks in order to improve voltage stability. Optimal placement of distributed generations (DGs) seems to be a viable solution for voltage stability enhancement of radial distribution networks.

The associate editor coordinating the review of this manuscript and approving it for publication was Jamshid Aghaei.

TABLE 1. List of abbreviation.

Symbol	Description	Symbol	Description
DG	Distributed Generation	$\Delta V, \Delta Q$	Change in voltage angle and reactive power.
P_{loss}	Total Active Power loss of network.	$APL,\ QPL$	Active and reactive power loss.
P_{ei},Q_{ei},V_i	Effective real and reactive power load and voltage at i^{th} bus.	λ_{max}	Maximum loadability of system.
VSI_i	Voltage stability index of i^{th} bus	$NVVB$	Total number of buses violating voltage limit.
$DVSI_{system}$	Distribution voltage stability index of system	VDI	The voltage deviation index
P^S_{grid}, Q^S_{grid}	Real and reactive power supplied by grid.	VPI	Voltage Profile Improvement index
$P_{load,i}$, $Q_{load,i}$	Real and reactive power load at i^{th}bus.	QLI	qualified load index
$P_{DG,i}$, $Q_{DG,i}$	Real and reactive power injected by DG at i^{th} node.	$APLR\%$, $QPLR\%$	Percentage active and reactive power loss reduction.
$P_{loss,i}$, $Q_{loss,i}$	Real and reactive power loss of i^{th}branch.	V_{min}, V_{max}	Minimum and maximum voltage of system.
I_i, R_i *and* $I_{i,max}$	Current, resistance and maximum current limit of i^{th} branch.	RDSs	Radial Distribution system.
b, nb	Number of nodes and closed branches in the system.	GWO.	Grey wolf optimization.
SW_i	Status of switch connected to i^{th} branch.	DV_R	Decision vector for reconfiguration.
A_{ij}	Elements of i^{th} row and j^{th} column of incidence matrix A.	DV_{RDG}	Decision vector for simultaneous reconfiguration and DG location and size.
TS_i, NTie	i^{th} tie switch and no. of tie switches.	DG_l	DG location.
FL_i	i^{th} Fundamental loop of network	DG_s	DG size
$\vec{A}$, $\vec{C}$, $\vec{a}$	Coefficient vectors. Coefficient of acceleration.	$DVPM$	Population matrix of Decision vector.
$\vec{P}_{prey}$, $\vec{P}_{wolf}$, $\vec{D}$	Position vector of the prey, and grey wolf. Distance between grey wolf prey.	$U_{min,x}$, $U_{max,x}$	Minimum and maximum value of decision variable x.
$\vec{r}_1$ *and* $\vec{r}_2$.	Random vectors in [0 1].	U^P_N	N^{th} decision variable in P^{th} row of Population matrix of decision variable.
t, T	current and maximum iterations count respectively.	APL_{old}, APL_{new}	Active power loss for base case and after Reconfiguration and or DG placement respectively.
Q_{L3}, Q_{SC3}, Q_3	Reactive power load, shunt capacitor injection in MVAr and net reactive power injection at bus 3 respectively.	QPL_{old}, QPL_{new}	Reactive power loss for base case and after Reconfiguration and or DG placement respectively.
ΔP_i, ΔQ_i, $\Delta\delta_i$, ΔV_i	Change in active power reactive power, voltage angle and magnitude of i^{th} bus.	V_i^{base}, $V_i^{REC/DG}$	Voltage magnitude of base case and after Reconfiguration and or DG placement of i^{th} bus respectively.
$\partial P_i/\partial\delta_j$, $\partial P_i/\partial V_j$, $\partial Q_i/\partial\delta_j$, $\partial Q_i/\partial V_j$	Real and reactive power sensitivity of i^{th} bus w.r.t. voltage angle and magnitude of j^{th} bus.	V_{limit}	Minimum or maximum voltage limit as case may be.
$V_{L,min}$, $V_{L,max}$	Minimum and maximum voltage limit respectively.	$P^{base}_{L,i}$	Real power load of i^{th} bus at base case.
CB_{ij}	Vectors of common branches in i^{th} and i^{th} FLs.	RG_i	Vectors of restricted group disconnecting common bus i.
P_0, Q_0	Initial active and reactive power.	P_{new}, Q_{new}	New active and reactive power at λ.
V^{old}_{min}	Minimum system voltage at previous λ	V^{new}_{min}	Minimum system voltage at increased λ

Fast Voltage Stability Index under varying load growth and penetration of wind and photo-voltaic have been reported for a practical Japanese distribution system to study its voltage stability enhancement [2]. Optimal placement of DGs based on Particle Swarm Optimization (PSO) has been considered for enhancement of maximum system loadability [8]. An ε-constraints based teaching and learning algorithm has been proposed to maximize system loadability and minimize losses under reconfiguration and DGs placement [9]. A probabilistic nature of renewable DG and load modeling has been studied to decide optimal location and size of DGs for voltage stability enhancement [10]. A new multi-objective index based optimization considering active and reactive power loss minimization in presence of DG unit has been proposed to enhance system loadability [11]. A voltage stability index driven optimal location of DG under increasing load has been reported for voltage stability improvement [12]. The hybrid differential evolutionary and particle swarm optimization approach has been reported to enhance the system loadability [13]. An analytical power stability index based DG placement algorithm has been proposed to realize the DG influence on loadability, network losses, and voltage magnitude [14]. An effective swarm-based optimization for DG placement has been reported to enhance voltage stability and reduce network losses [15], [16]. Placement of permanently connected capacitor wind-operated squirrel cage induction based dispersed generator has been performed to enhance voltage stability [17].

Network reconfiguration is another important strategy that is being utilized for performance enhancement of distribution networks through closing and opening the sectionalizers and/or tie lines. In general, distribution system constitutes a mix of residential, commercial, industrial types of loads. The feeder of these systems may experience variable load patterns at different time frame with changing days and seasons. At some point of time the system is loaded heavily while at another time it is lightly loaded. In such a scenario, load scheduling by reconfiguration may lead to optimal performances with regard to system losses and voltage stability. Reconfiguration of radial network smoothens peak demands

that improves the voltage profile, and maximum loadability thus making the network quite reliable [18]. Optimal reconfiguration with different optimization techniques have been reported to enhance the system loadability [19]–[23]. A fuzzy genetic rule-based optimization for reconfiguration is studied to enhance voltage stability [24]. A discrete artificial bee colony approach is adopted based on Continuation Power Flow algorithm to enhance maximum loadability of system [25], [26]. A two-stage algorithm for reactive power loss minimization to enhance voltage stability and loadability enhancement through network reconfiguration has been proposed [27]. A two stage hierarchical optimization approach has been presented to tradeoff between enhanced maximum loadability and reduced network losses under reconfigurable [28] and integrable DG environment [29], [30]. The matroid theory based reconfiguration was carried out with the help of graph theory [31].

In traditional transmission and distribution systems, presence of PV and PQ buses is very common. Static voltage stability analysis has been carried out by introducing novel bus type referred as bus AQ with known reactive power demand and bus voltage angle [32]. Thus, voltage magnitude and real power at AQ bus remain unknown. In recent publications, the concept of voltage control at PQV buses by remotely located P buses has been introduced. The dedicated P bus having pre-defined real power injection has variable reactive power source that controls the voltage of PQV bus [33]–[35]. A PQV bus is defined as the bus with pre-specified quantities of active power, reactive power and voltage magnitude. Only the voltage angle of this bus is unknown. A P bus is defined as a reactive power generator bus which is maintaining the voltage magnitude at PQV bus constant at the required value [33]. For a P bus, the quantity of active power is pre-specified. The quantities reactive power, voltage magnitude and voltage angle at this bus remain unknown and hence need to be calculated. Injection of regulated reactive power at generator bus P results in maintaining the desired value of the voltage magnitude of PQV bus located remotely [34]. The PQV bus thus has pre-defined voltage magnitude in addition to pre-defined real and reactive power injections. Loss minimization under reconfigurable and optimally integrated DG environment has been performed in a system employed with remotely located PQV bus with its voltage magnitude being maintained by variation of reactive power injection at the selected P bus [36], [37]. The bus with minimum voltage magnitude has been chosen as PQV bus while P bus was selected by choosing the bus which gives least power loss in the network.

Literature review reveals that loadability enhancement of distribution system has been studied so far by various authors under presence of PQ buses in the system. Maintenance of voltage at a remote PQV bus through variation of reactive power injection at P bus may be quite helpful in enhancing maximum loadability of the system. Optimal placement of DGs and network reconfiguration under presence of PQV and P buses may further enhance voltage stability margin. No effort seems to be made in study of loadability enhancement through network reconfiguration and DG placement under presence of PQV and P buses. In order to overcome this research gap, this paper proposes a multi-objective fitness function to enhance maximum loadability and reduce network losses by reconfiguration and DG unit allocation under presence of P and PQV buses in the system. The fitness function has been optimized through Grey Wolf Optimization (GWO) technique. Maximum loadability obtained by proposed approach has been compared with existing approaches to establish its effectiveness.

II. PROBLEM FORMULATION: OBJECTIVE FUNCTION AND CONSTRAINTS

In this work network reconfiguration and DG allocation has been performed for a certain designed set of objective functions. To achieve the optimum solution space with the optimum objective, the Grey Wolf Optimization tool has been implemented. Real power loss minimization is the main factor that distribution companies want to perform since this objective is not only economically favorable to distribution companies worldwide but also it enhances the operational constraints of the distribution system. Apart from this increasing load demand restricts the distribution system planners to operate it within the stable region, beyond a particular load the network does not remain stable and becomes unstable. To accomplish the increased load demand and stable system operation voltage stability or loadability limit of the system must be incorporated in the objective problem formulation and hence a distribution system voltage stability index has been formulated.

The Objective Functions are

$$f_1 = P_{loss} = \sum_{i=1}^{b} sw_i[I_i^2 R_i] \tag{1}$$

where sw_i is the status of i^{th} branch, sw_i=0 if the switch is open and sw_i=1, if it is closed, P_{loss} is total network real power loss i.e. sum of losses in all closed branches, I_i is current flowing in i^{th} branch and R_i is the resistance of i^{th} branch, and b represents total number of closed branches.

$$f_2 = DVSI_{system} = \sum_{i=1}^{nb}[VSI_i] \tag{2}$$

where,

$$VSI_i = |V|_{i-1}^4 - 4(P_{ei}X_i - Q_{ei}R_i)^2 - 4(P_{ei}R_i - Q_{ei}X_i)|V|_{i-1}^2 \quad \forall i \in [2,\ nb][21] \tag{3}$$

$DVSI_{system}$ represents voltage stability index of whole distribution system. Determination of VSI_i is explained by means of a simple distribution network shown in Figure 1. In Figure 1, P_{ei} and Q_{ei} represents effective real and reactive power demand at i^{th} bus in two bus equivalent network [21], X_i represents reactance of i^{th} closed branch and nb represents total number of buses present in the system.

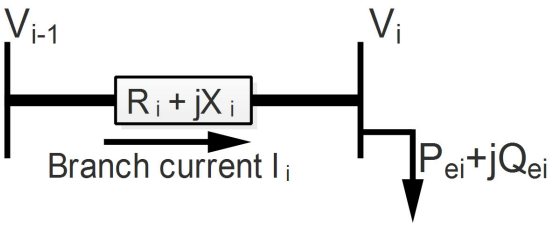

FIGURE 1. Simple distribution network line.

The effective load P_{ei} (Q_{ei}) at i^{th} bus can be evaluated by addition of all real (reactive) demands at i^{th} bus and all other buses beyond i^{th} bus and the addition of real (reactive) losses incurred across all the branches beyond i^{th} bus.

Minimization of a multi-objective problem formulation has been proposed in this work that considers minimization of network losses and maximization of voltage stability. The proposed multi-objective function is given as:

$$f = w_1 f_1 - w_2 f_2 \tag{4}$$

$$s.t.\ (w_1 + w_2) = 1 \tag{5}$$

where, w_1 and w_2 represents weightage assigned to f_1 and f_2, respectively. To convert the maximization optimization formulation into minimization negative sign has been assigned to the objective function, f_2.

The constraints are:

Power balance constraints:

$$P^s_{grid} + \sum_{i=1}^{NDG} P_{DG,i} = \sum_{i=1}^{nb} P_{load,i} + \sum_{i=1}^{b} P_{loss,i} \tag{6}$$

$$Q^s_{grid} + \sum_{i=1}^{NDG} Q_{DG,i} + Q_{sh,i} = \sum_{i=1}^{nb} Q_{load,i} + \sum_{i=1}^{b} Q_{loss,i} \tag{7}$$

where,

P^s_{grid} = Real power injected through grid to the radial distribution network

Q^s_{grid} = Reactive power injected through grid to the radial distribution network

$P_{DG,i}$ = real power injected to the network through DG placed at bus-i

$Q_{DG,i}$ = reactive power injected to the network through DG placed at bus-i

$Q_{sh,i}$ = reactive power injected to the network through shunt capacitor placed at bus-i

NDG = total number of DGs placed in the system

$P_{load,i}$ = real power demand at bus-i

$Q_{load,i}$ = reactive power demand at bus-i

$P_{loss,i}$ = real power loss in closed branch i

$Q_{loss,i}$ = reactive power loss in closed branch i

DG Size constraint:

$$\sum_{i=1}^{NDG} P_{DG,i} \le \sum_{i=1}^{nb} P_{load,i} + \sum_{i=1}^{b} P_{loss,i} \tag{8}$$

The bus voltages should be within permissible limits:

$$V_{L,min} \le V_i \le V_{L,max} \tag{9}$$

where, V_i is i^{th} bus voltage magnitude, $V_{L,max}$ and $V_{L,min}$ represents maximum and minimum voltage limits. In this work $V_{L,max}$ and $V_{L,min}$ has been taken as 1.05 pu and 0.95 pu respectively, considering beyond $\pm 5\%$ voltage variation as large voltage variations.

Current in each branch should be within the permissible limit

$$I_k \le I_{k,max} \quad \forall k = 1, 2, \ldots b \tag{10}$$

where, $I_{k,max}$ represents maximum permissible current in branch k.

To operate the system radially, equality constraint required is as below:

$$nb = b + 1 \tag{11}$$

III. REFORMULATION OF NRLF EQUATION UNDER PQV AND P BUSES

Existence of pair of PQV and P buses in network may be solved by redefining the Jacobian matrix. A P bus is introduced as a reactive power source with unknown reactive power output [33]. Since the P bus with unspecified reactive source injection Q controls the voltage magnitude of remotely located PQV bus, hence this unknown quantity Q becomes the state variable, while real power generation at P bus is set to zero. A PQV bus has the characteristics of a PQ bus with known voltage magnitude in addition to real and reactive power injections [33]. By injecting the appropriate amount of reactive power at P bus, the desired magnitude of voltage at PQV bus is achieved. The detailed explanation regarding concept of PQV and P buses has been illustrated by means of a simple 5 bus system shown in Figure 2. In Figure 2, bus 1 is set to be a reference bus, buses 2 and 4 are assigned as PQ bus while buses 3 and 5 have been designated as P and PQV bus, respectively. To incorporate the concept of the P bus (bus 3) to keep the magnitude of voltage of the PQV bus (bus 5) constant, set of equations augmented are given by (12) and (13) as below:

$$\Delta V = [\Delta V_2 \quad \Delta V_3 \quad \Delta V_4]^T \tag{12}$$

$$\Delta Q = [\Delta Q_2 \quad \Delta Q_4 \quad \Delta Q_5]^T \tag{13}$$

With the above modification, equation augmented relating to power mismatch with respect to the mismatch in the phase angle and voltage magnitudes for the Newton-Raphson algorithm takes the form as below:

$$Y = JX \tag{14}$$

where,

$$Y = [\Delta P_2\ \Delta P_3\ \Delta P_4\ \Delta P_5\ \Delta Q_2\ \Delta Q_4\ \Delta Q_5]^T$$

$$X = [\Delta \delta_2\ \Delta \delta_3\ \Delta \delta_4\ \Delta \delta_5\ \Delta V_2\ \Delta V_3\ \Delta V_4]^T$$

and J, as shown at the bottom of the next page.

With the above modification in the power balance equation, the Newton Raphson load flow method solves the network for unknown reactive injection (Q_3) at bus P and other state variables. To keep the voltage of PQV bus constant, different voltage controlling devices given in [34] may be utilized. In this work the desired PQV bus voltage is achieved by assuming a shunt capacitor placed at P bus due to its low cost as compared to other voltage controlling devices.

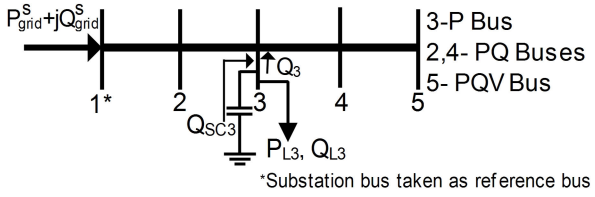

FIGURE 2. Simple 5 bus network with different types of buses with shunt capacitor injection.

In Figure 2, Q_{SC3} represents the amount of reactive power injection by the shunt capacitor Placed at P bus 3 to maintain voltage of PQV bus 5 constant. Once the net reactive power injection Q_3 at bus 3 is obtained using (14) in load flow, the value of reactive power Q_{SC3} requisite at P bus 3 to keep the voltage magnitude constant at PQV bus 5 is computed using the formula (15), given below:

$$Q_{SC3} = Q_3 + Q_{L3} \tag{15}$$

where, Q_3 = net reactive power injection at bus 3.

Q_{SC3} = reactive power injection by shunt capacitor at bus 3.

Q_{L3} = specified reactive power load at bus 3.

IV. SOLUTION METHOD FOR THE RECONFIGURATION

In this section concept of network reconfiguration as a decision variable has been explained.

A. RECONFIGURATION USING FUNDAMENTAL LOOPS METHOD AND ITS DEMERITS

In a radial distribution system (RDS),there are certain number of initially opened tie-switches and normally closed branches, in general. These normally closed branches are equipped with sectionalizer switches. Closing these tie-switches creates many numbers of loops in the system. To reconfigure the distribution system, associated sectionalizer switches of a set of particular branches in association with the available tie-switches must be opened and closed. Selection of these switches to alter the topology of network is a tedious and cumbersome job as there are huge number of possible combinations of switches. Generally, a random selection of these switches is done. To generate the random initial population meta-heuristic methods have been proposed. Thus, a random selection of these switches in decision variable population creates large number of network configurations many of which, may violate radial topology constraints as well as load bus disconnection while dealing with distribution network reconfiguration problem leading to infeasibility. Fundamental loop (FL) analysis is a viable and suggested solution to reduce this tedious job with a certain extent [38]. Selection of random switches in decision variable is now made only with associated fundamental loop. Fundamental loop analysis using graph theory, not only ascertains the reduction in search space of network configuration but also elimination of many infeasible population generations. Total number of fundamental loops (nFL) present in a RDS is obtained using (16) given below:

$$nFL = NTie + b - nb + 1 \tag{16}$$

Total number of FLs in a RDS is same as the number of available tie-switches, NTie. Each FL has constituent branches and tie-switches associated with it. To determine the constituent/members of FLs, each loop-forming branch has been selected including tie-switch closed to form the loop.

$$J = \begin{bmatrix} \frac{\partial P_2}{\partial \delta_2} & \frac{\partial P_2}{\partial \delta_3} & \frac{\partial P_2}{\partial \delta_4} & \frac{\partial P_2}{\partial \delta_5} & \frac{\partial P_2}{\partial V_2} & \frac{\partial P_2}{\partial V_3} & \frac{\partial P_2}{\partial V_4} \\ \frac{\partial P_3}{\partial \delta_2} & \frac{\partial P_3}{\partial \delta_3} & \frac{\partial P_3}{\partial \delta_4} & \frac{\partial P_3}{\partial \delta_5} & \frac{\partial P_3}{\partial V_2} & \frac{\partial P_3}{\partial V_3} & \frac{\partial P_3}{\partial V_4} \\ \frac{\partial P_4}{\partial \delta_2} & \frac{\partial P_4}{\partial \delta_3} & \frac{\partial P_4}{\partial \delta_4} & \frac{\partial P_4}{\partial \delta_5} & \frac{\partial P_4}{\partial V_2} & \frac{\partial P_4}{\partial V_3} & \frac{\partial P_4}{\partial V_5} \\ \frac{\partial P_5}{\partial \delta_2} & \frac{\partial P_5}{\partial \delta_3} & \frac{\partial P_5}{\partial \delta_4} & \frac{\partial P_5}{\partial \delta_5} & \frac{\partial P_5}{\partial V_2} & \frac{\partial P_5}{\partial V_3} & \frac{\partial P_5}{\partial V_5} \\ \frac{\partial Q_2}{\partial \delta_2} & \frac{\partial Q_2}{\partial \delta_3} & \frac{\partial Q_2}{\partial \delta_4} & \frac{\partial Q_2}{\partial \delta_5} & \frac{\partial Q_2}{\partial V_2} & \frac{\partial Q_2}{\partial V_3} & \frac{\partial Q_2}{\partial V_5} \\ \frac{\partial Q_4}{\partial \delta_2} & \frac{\partial Q_4}{\partial \delta_3} & \frac{\partial Q_4}{\partial \delta_4} & \frac{\partial Q_4}{\partial \delta_5} & \frac{\partial Q_4}{\partial V_2} & \frac{\partial Q_4}{\partial V_3} & \frac{\partial Q_4}{\partial V_5} \\ \frac{\partial Q_5}{\partial \delta_2} & \frac{\partial Q_5}{\partial \delta_3} & \frac{\partial Q_5}{\partial \delta_4} & \frac{\partial Q_5}{\partial \delta_5} & \frac{\partial Q_5}{\partial V_2} & \frac{\partial Q_5}{\partial V_3} & \frac{\partial Q_5}{\partial V_5} \end{bmatrix}$$

The incidence matrix 'A', is generated using the graphical method representation of RDS [39]. The size of matrix 'A' is b × nb. The element A_{ij} in matrix 'A' is obtained using expression (17):

$$A_{ij} = \begin{cases} 1, & \text{if branch i is away from } j^{th} \text{ bus} \\ -1, & \text{if branch i is incident to } j^{th} \text{ bus} \\ 0, & \text{otherwise} \end{cases} \quad (17)$$

To obtain the first FL, an open branch containing the first tie-switch is inserted into the incidence matrix 'A'. The sum of the absolute value of each element in each column of matrix 'A' is evaluated. Buses which have the sum equals to 1 are identified. Branches connected to these buses are removed. The procedure is repeated until the sum result in no longer equal to 1. A vector is formed to store the remaining branches in matrix 'A' representing first FL. The remaining FLs are determined using the same procedure as the first FL [40].

For a system having NTie tie-switches, the required length of the decision vector becomes equal to NTie as each switch is selected from each fundamental loop. Hence, the decision

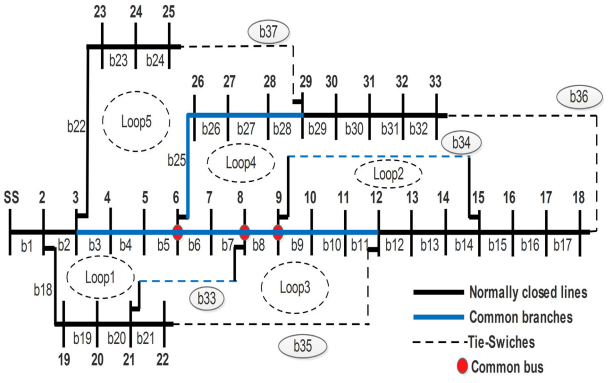

FIGURE 3. Schematic of 33 bus radial distribution.

variables in this system are represented by actual branch/tie number as

$$DV_R = [TS_1, TS_2, \ldots, TS_{NTie}] \quad (18)$$

where, TS_i is the branch/tie-switch to be opened in the i^{th} fundamental loop created by closing the tie switch associated with the loop. To illustrate this, Figure 3 with schematic of the IEEE 33-bus distribution system is shown. In Figure 3, the digits 1, 2, 3, etc., represent the bus numbers, while the branches (switches) are numbered as b1, b2, b3, ...etc. Total five number of tie switches represented as b33, b34, b35, b36, and b37, forming five fundamental loops are present in this system. Details of these loops are also presented in Table 2.

However, selection of switches from each fundamental loop has its own demerits. Certain combinations of selected switches from each fundamental loop may isolate one or more system buses in radial distribution system. For simple understanding, consider the IEEE 33-bus distribution network shown in Figure 3. Let us suppose decision variable [b6 b14 b21 b7 b22] generated with the selection of one switch from each fundamental loop. If this decision variable is selected, then load bus 6 will be isolated as both b6 and b7 belongs to fundamental loops 1 and 4. Both these branches are common to fundamental loops 1 and 4 and hence participation of such common branches between two loops must be restricted to only one in either loop. There are many more such combinations that exist between any two loops. Let us take another combination of switches [b6 b34 b8 b25 b5] selected from each fundamental loop. Opening of these switches isolate the load bus 6 from the distribution system. This is because of bus 6, which is common to fundamental loops 1, 4 and 5 and branches b6, b25 and b5 common between two loops participating simultaneously. To overcome these demerits, each combination of decision variable for reconfiguration must adhere to a set of rules designed. And hence, the concept of switch selection from each fundamental loop needs to be modified based on certain rules.

TABLE 2. Fundamental loops for the IEEE 33-bus system.

FL	Switches (Tie/sectionalizer)	Tie Switch	Length of FL
1	b2, b3, b4, b5, b6, b7, b18, b19, b20, b33	b33	10
2	b9, b10, b11, b12, b13, b14, b34	b34	7
3	b8, b9, b10, b11, b33, b21, b35	b35	7
4	b25, b26, b27, b28, b29, b30, b31, b32, b36, b15, b16, b17, b34, b6, b7, b8	b36	16
5	b3, b4, b5, b22, b23, b24, b25, b26, b27, b28, b37	b37	11

B. RULE BASED DECISION VARIABLES MODIFICATION

Each decision variable must have NTie number of elements, representing the number of switches to be opened to operate system in a radial manner. To incorporate the demerits of fundamental loops reported in previous sub-section the set of rules defined are as below:

Rule-1 : At least one element must be chosen from each fundamental loop. $TS_i \in FL_i$.

Rule-2 : If a common branch vector participates while creating a decision variable, it must be ensured that at most a single element is chosen.

Rule-3 : While creating a decision variable it must be ensured that all the vectors with common branches of any restricted group must avoid the simultaneous participation.

To form the feasible decision variables, algorithm are explained as below [41]:

Step 1 : Create fundamental loop vectors, having the set of switches in each fundamental loop, as shown in Table 2.

Step 2 : Obtain the decision variable such that TS_i belonging to FL_i following the 1^{st} Rule.

Step 3 : Obtain vectors of common branches, CB_{jk}, having the set of switches common between two loops FL_j and FL_k.

Step 4 : Obtain vectors of restricted group RG_i, cluster of common branch vectors incident at the i^{th} common bus(es) of the distribution network.

Step 5 : Check and modify the decision variable to satisfy the feasibility based on the 1^{st}, 2^{nd} and 3^{rd} rules designed.

The first rule ensures the selection of switches to be opened from each fundamental loop and prevention of any load bus disconnection at the exterior of the network, while 2^{nd} and 3^{rd} rules prevent the disconnection of the load buses at the interior of the network. Hence, these rules ensure the generation of feasible decision variables with radiality of the network as well as prevention of any bus disconnection. In this work, GWO is adapted using basics of graph theory to populate the decision variables. The GWO guided by set of rules defined above modifies the infeasible decision variable into feasible one during iteration process. This algorithm bypasses the hectic mesh check and overcomes the deficiency of the reconfiguration method by [38]–[40] to create feasible decision variables. To understand the algorithm for reconfiguration, let us consider the IEEE 33-bus network, shown in the Figure 3.

TABLE 3. Vectors of common branches.

Vectors of Common Branches	
CB_{13} = [b33]	CB_{24} = [b34]
CB_{14} = [b6 b7]	CB_{34} = [b8]
CB_{15} = [b3 b4 b5]	CB_{45} = [b25 b26 b27 b28]
CB_{23} = [b9 b10 b11]	

TABLE 4. Vectors of restricted group.

Vectors of Restricted Group	common bus(es) disconnected
$RG_6 = [CB_{14}\ CB_{15}\ CB_{45}]$	6
$RG_8 = [CB_{13}\ CB_{14}\ CB_{34}]$	8
$RG_9 = [CB_{23}\ CB_{34}\ CB_{24}]$	9
$RG_{68} = [CB_{13}\ CB_{15}\ CB_{34}\ CB_{45}]$	6,8
$RG_{89} = [CB_{13}\ CB_{14}\ CB_{23}\ CB_{24}]$	8,9
$RG_{689} = [CB_{13}\ CB_{15}\ CB_{23}\ CB_{24}\ CB_{45}]$	6,8,9

The list of vectors of common branches between two fundamental loops, obtained from Figure 3, are presented in Table 3. The restricted group vectors and the associated common buses that may be disconnected, if all the common branch vector participate in decision variable creation for the system are obtained from Figure 3, as shown in Table 4. For the distribution system shown in Figure 3, The decision variable constitutes total five switches selected from each fundamental loop according to 1^{st} Rule. Suppose the decision variable [b20 b13 b35 b26 b25] is populated at any instant of iteration. It can be observed that this decision variable is violating the 2^{nd} rule as both b26 and b25 switches belong to CB_{45}. If this decision variable is selected, then load bus 26 will be isolated. Let us Consider another infeasible decision variable [b7 b34 b8 b25 b4], violating the 3^{rd} Rule, since switches b7, b25, b4 belong to vector of common branches CB_{14}, CB_{45} and CB_{15} respectively, which falls under the vectors of restricted group $RG_6 = [CB_{14}\ CB_{15}\ CB_{45}]$ isolating common bus 6. Selecting switches for reconfiguration creates many more infeasible decision variables which can be converted into feasible ones in accordance with 1^{st}, 2^{nd} and 3^{rd} Rules. To demonstrate the modification of infeasible decision variable into the feasible decision variable under the guidance of vectors of common branches and restricted groups are shown in Figure 4 through an example. As shown in Figure 4 decision variable [b20 b13 b35 b26 b25] populated at any stage of iteration, violates the 2^{nd} Rule. According to 2^{nd} Rule switches [b25 b26 vb27 b28], which belong to CB_{45} and hence only one switch has to participate either in 4^{th} or 5^{th} fundamental loop from this vector. Therefore, 4^{th} loop switch is modified under the guidance of 1^{st}, 2^{nd} and 3^{rd} Rules replacing the switch b25 by b29 creating a feasible decision variable [b20 b13 b35 b29 b25].

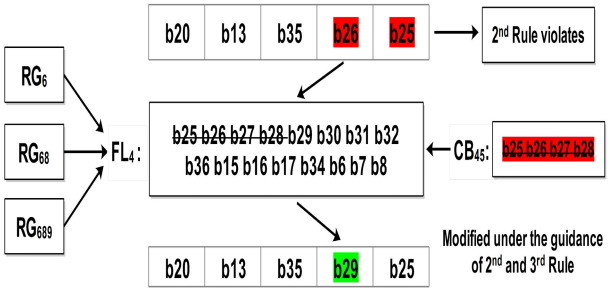

FIGURE 4. Modification of decision variable.

V. GREY WOLF OPTIMIZATION SEARCH ALGORITHM: AN OVERVIEW

Like other evolutionary ones, this algorithm model the hunting behavior of grey wolves and starts with an initial population of these hunting wolfs. Population individuals called wolf are subdivided into alpha beta, delta, and omega wolf. These wolves attack the prey based on their location and distance from the prey. Encircling, hunting, and attacking the prey are the three important steps for prey hunting [42].

A. ENCIRCLING

Encircling of the prey by the grey wolf is modeled as;

$$\vec{D} = |\vec{C} \cdot \vec{P}_{prey}(t) - \vec{P}_{w}(t)| \tag{19}$$

$$\vec{P}_{wolf}(t+1) = \vec{P}_{prey}(t) - \vec{A} \cdot \vec{D} \tag{20}$$

where, $\vec{D}$ is the distance between grey wolf and prey, $\vec{A}$ and $\vec{C}$ are coefficient vectors, $\vec{P}_{prey}$ is the position vector of the prey, and $\vec{P}_{wolf}$ indicates the position vector of a grey wolf. The coefficient vectors $\vec{A}$ and $\vec{C}$ are given by;

$$\vec{A} = 2\vec{a} \cdot \vec{r}_1 - \vec{a} \tag{21}$$

$$\vec{C} = 2\vec{r}_2 \tag{22}$$

where, coefficient of acceleration $\vec{a}$ is decreased linearly from 2 to 0 throughout the iterations. $\vec{r}_1$ and $\vec{r}_2$ are random

vectors in [0 1]. During the encircling the prey changes its position and try to get away from the wolves, vectors $\overrightarrow{A}$ and $\overrightarrow{C}$ updates the position of a wolf according to that of changing the position of the prey [42] and brings the position of the wolf closer to prey.

B. HUNTING

The alpha wolf is superior to the entire wolves and leads the hunting of prey in association with beta and delta wolves. The beta and delta wolf follows the alpha wolf in hunting. To represent the hunting phenomena during the iteration process, the best candidates considered first as solutions are alpha, beta, and delta wolves. The fourth search agent i.e. omega wolves update their positions in association with and according to the best search solution obtained from alpha, beta, and delta wolves. Mathematically this can be modeled as:

$$\overrightarrow{P}_{wolf}(t+1) = \frac{\overrightarrow{P}_1 + \overrightarrow{P}_2 + \overrightarrow{P}_3}{3} \tag{23}$$

$$\left.\begin{aligned} \overrightarrow{D}_\alpha &= |\overrightarrow{C}_1 \overrightarrow{P}_\alpha - \overrightarrow{P}_{wolf}|; \\ \overrightarrow{D}_\beta &= |\overrightarrow{C}_2 \overrightarrow{P}_\beta - \overrightarrow{P}_{wolf}|; \\ \overrightarrow{D}_\delta &= |\overrightarrow{C}_3 \overrightarrow{P}_\delta - \overrightarrow{P}_{wolf}| \end{aligned}\right\} \tag{24}$$

$$\left.\begin{aligned} \overrightarrow{P}_1 &= \overrightarrow{P}_\alpha - \overrightarrow{A}_1.\overrightarrow{D}_\alpha; \\ \overrightarrow{P}_2 &= \overrightarrow{P}_\beta - \overrightarrow{A}_2.\overrightarrow{D}_\beta; \\ \overrightarrow{P}_3 &= \overrightarrow{P}_\delta - \overrightarrow{A}_3.\overrightarrow{D}_\delta \end{aligned}\right\} \tag{25}$$

C. ATTACKING

In this phase, the wolves take the position of prey without letting the prey to change its position and assault it. The vector coefficient $\overrightarrow{A}$ in mathematical modeling depicts the approach of the victim and plays a key role and its vacillation range gradually reduces by acceleration coefficient vector $\overrightarrow{a}$ as the wolf moves closer to the prey. In general, vector $\overrightarrow{A}$ changes its value in the interval [-a a] randomly, and is governed by decreasing the value of the vector $\overrightarrow{a}$ from 2 to 0 linearly throughout the iterative process. During the attack modeling the position of a solution candidate, the succeeding location/position of a candidate solution/wolf will be somewhere in between its current location and the location of prey, if the random value of the vector $\overrightarrow{A}$ lies in the range[-1 1]. The absolute value of the vector $\overrightarrow{A}$ ensures the convergence of the solution candidate if it satisfies (26); otherwise, there is no solution as the candidate diverges away from the prey if the absolute value follows (27), and definitely, an optimally best prey will be evolved as a final solution with this algorithm.

$$\text{Solution converges if } |A| < 1 \tag{26}$$

$$\text{Solution diverges if } |A| \geq 1 \tag{27}$$

D. ACCELERATION COEFFICIENT

The acceleration coefficient vector $\vec{a}$ controls the exploration and exploitation process and balances it with adequate value. A larger surface area for exploration results in sluggishness and the increased chance of stagnation to be trapped in local optima, and hence an enhanced rate of exploration can be achieved by decreasing the acceleration coefficient vector linearly with increasing iterations, where the acceleration coefficient is varied adaptively throughout the iterations and is given as;

$$a = 2(1 - \frac{t}{T}) \tag{28}$$

where, t and T are current and maximum iterations count respectively, during the optimization process adopted.

VI. PROPOSED GWO BASED ALGORITHM FOR MULTI-OBJECTIVE FUNCTION

The illustration of the GWO algorithm application for the reconfiguration of the distribution system by closing/opening of branch/tie switches to evaluate the objective function is presented in this section. In this work, a number of cases that consist of reconfiguration with and without simultaneous allocation of single DG injecting only real power are taken to minimize the objective function using GWO. To reconfigure the distribution system, variables of decision vector DV_R are same as the total number of loops (represented by a discrete variable) present in the system as below:

$$DV_R = [TS_1, TS_2, \ldots.., TS_{NTie}] \tag{29}$$

However, for the application of simultaneous DG allocation and reconfiguration, the length of decision variables in the decision vector DV_{RDG} are equivalent to the addition of elements in DV_R and double the number of DG, each for DG position (discrete variable DG_l) and DG size (continuous variable DG_s) as represented below:

$$DV_{RDG} = \begin{bmatrix} TS_1, TS_2, \ldots TS_{NTie} & DG_l & DG_s \\ \text{Tie switches number} & \text{DG loacation} & \text{DG size} \end{bmatrix} \tag{30}$$

For better understanding, further the variables either for switches, location and size will be denoted as $U_x (x = 1, 2, 3, \ldots, N)$. This notation will be used for optimal switches, location and size of DG positions to evaluate the fitness function.

In the start, GWO optimization parameters are assigned and a DVPM is created. Every row of DVPM is denoted by a decision vector. The elements of the $DV_R(U_x)$ is generated using (31) as shown below:

$$U_x^k = U_{min,x} + rand(U_{min,x} - U_{max,x}) \tag{31}$$

The population matrix of decision vectors is generated using (31) as shown below:

$$DVPM = \begin{bmatrix} U_1^1 & U_2^1 & U_3^1 & \ldots & U_{N-1}^1 & U_N^1 \\ U_1^2 & U_2^2 & U_3^2 & \ldots & U_{N-1}^2 & U_N^2 \\ \cdot & \cdot & \cdot & \cdot & \cdot & \cdot \\ \cdot & \cdot & \cdot & \cdot & \cdot & \cdot \\ U_1^{P-1} & U_2^{P-1} & U_3^{P-1} & \ldots & U_{N-1}^{P-1} & U_N^{P-1} \\ U_1^P & U_2^P & U_3^P & \ldots & U_{N-1}^P & U_N^P \end{bmatrix} \tag{32}$$

In GWO the decision vector represents the grey wolf. Corresponding to grey wolf evaluated fitness function given by (4) represents the position of prey.

The flowchart for proposed GWO based stability enhancement approach under optimal DG placement, network reconfiguration and presence of PQV and P buses is shown in Figure 5. As per this flowchart maximum loadability of the system is computed under optimal fitness function and decision variables, where decision variables consist of open status of tie switches and DG location and size.

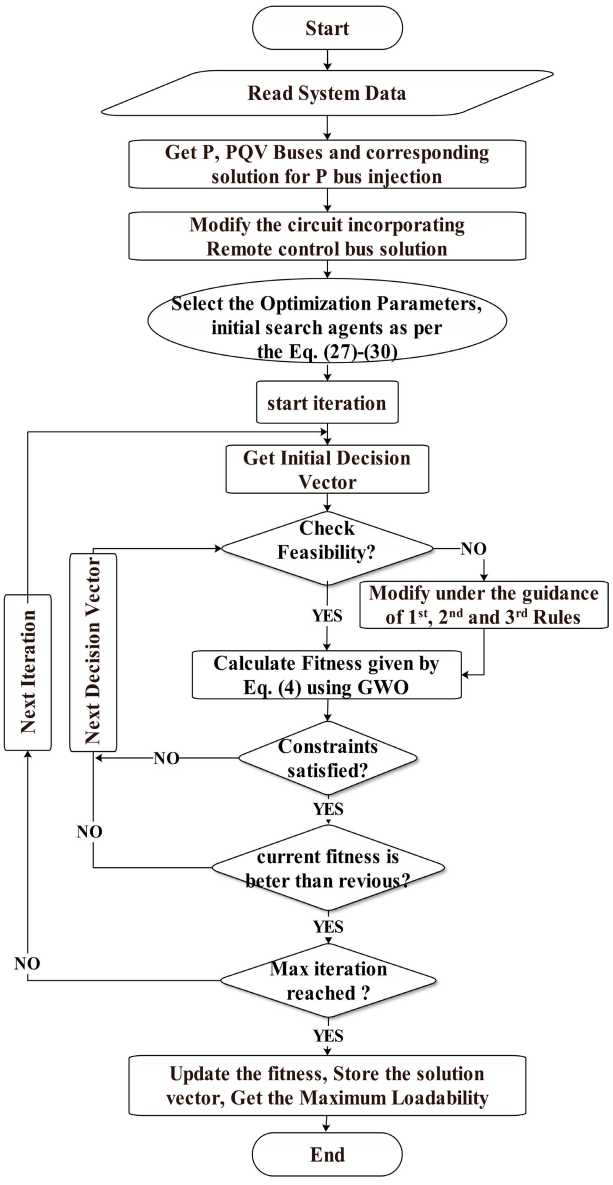

FIGURE 5. Flowchart for minimization of multi-objective fitness function using GWO algorithm.

A. MAXIMUM LOADABILITY CALCULATION

In voltage stability analysis, one of the most significant part is the determination of maximum system loadability. Considering a load case, a successive load flow utilizes the network solution to evaluate the minimum voltage magnitude till the collapse point (i.e., where the load flow solution diverges) to evaluate the voltage stability margin [5] and to draw the loadability curve. The voltage stability margin is calculated in terms of maximum loadability. The voltage stability margin is termed as the extent from an operating point to a voltage collapse point until the load increment can be served without fail. In the successive procedure, the active and reactive load power at each bus in the system is increased repeatedly by a loading factor λ given by:

$$P_{new} = P_0(1 + \lambda) \tag{33}$$

$$Q_{new} = Q_0(1 + \lambda) \tag{34}$$

where, P_0 and Q_0 are the active and reactive power loads at initial operating point, and P_{new} and Q_{new} are new active and reactive power demand at loading factor λ which is increased at a rate of 1%.

Voltage stability margin has been defined as the distance between initial operating point (loading factor $\lambda = 0$) to maximum loadability point having loading factor as λ_{max}. Maximum loadability point has been obtained based on the divergence of load flow. Voltage stability margin has been shown in Figure 6 representing loading factor, λ Vs. voltage magnitude curve for the system. The flow chart in Figure 7 presents the algorithm to calculate the maximum loadability.

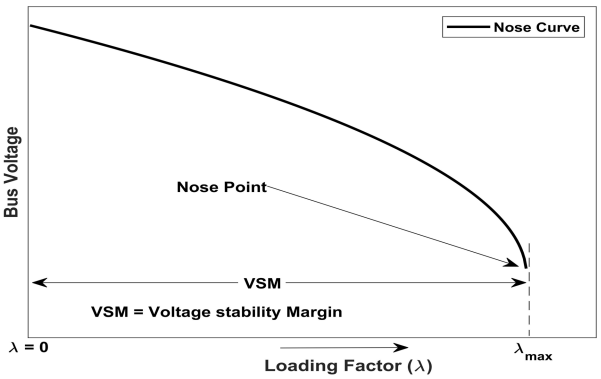

FIGURE 6. Flow chart for determination of maximum loadability.

The following six cases have been studied to examine impact of DG allocation, network reconfiguration and presence of PQV and P buses in voltage stability margin (maximum loadability) enhancement.

Case 1 : It is a case study of base-case without considering reconfiguration and PQV and P buses.

Case 2 : It is an application of only network reconfiguration without consideration of PQV and P buses.

Case 3 : It is the case study for simultaneous reconfiguration and DG allocation without PQV and P buses.

Case 4 : It is a case study when PQV and P buses have been considered for base case.

Case 5 : It is a case study when PQV and P buses have been considered for reconfiguration only.

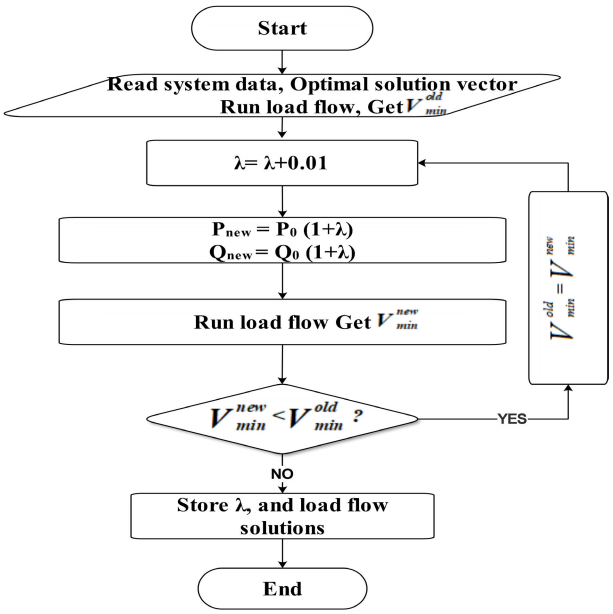

FIGURE 7. Flow chart for determination of maximum loadability.

Case 6 : It is the case for simultaneous reconfiguration and DG allocation with consideration of PQV and P buses.

VII. INDICES TO EXAMINE SYSTEM PERFORMANCE

To analyze the effects of reconfiguration and/or DG placement, different performance indices [9] have been evaluated. These indices are defined as below:

1) NUMBER OF VOLTAGE LIMIT VIOLATING BUSES (*NVVB*)

NVVB signifies the number of buses violating the permissible voltage limits in the system considered.

2) VOLTAGE DEVIATION INDEX (*VDI*)

In order to specify the measure of violation of limits imposed on voltage magnitudes at buses in an *nb* bus system, the voltage deviation index (*VDI*) is defined as:

$$VDI = \sqrt{\frac{(\sum_{i=1}^{NVVB}(V_i - V_{limit})^2)}{nb}} \tag{35}$$

where, i belong to set of buses violating upper or lower voltage limit.

V_i = voltage magnitude at bus i.

$V_{i,limit}$ = upper or lower voltage limit at bus i.

nb = total number of buses present in the system. During reconfiguration and DG placement, *VDI* signifies the amount of voltage fluctuation at buses violating voltage limits. It is desired to have zero voltage deviation index (*VDI*),i.e. voltage at all buses should be within permissible limits.

3) VOLTAGE PROFILE IMPROVEMENT INDEX (*VPI*)

$$VPI = \sqrt{(\sum_{i=1}^{nb}(V_i^{base} - V_i^{REC/DG})^2)pu} \tag{36}$$

In a radial distribution system at base load condition, the voltage at source to remote buses falls much below the desired 1 pu value, due to voltage drops in lines. With the incorporation of distributed generation and/ or tie-switch allocation the voltage at each bus changes to different operating value. Incorporation of these devices in system leads to further rise or drop in voltages leading to improvement or deterioration in voltages at a specific or set of buses in the network. Hence, voltage profile improvement index (*VPI*) signifies the appropriate selection of these devices (Reconfiguration and DG placement considered in our work) for enhancement of the voltage profile of the network.

4) QUALIFIED LOAD INDEX (*QLI*)

Qualified load index is defined as:

$$QLI = \sum_{i=1}^{nb} V_i P_{L,i}^{base} \tag{37}$$

where, V_i = voltage at bus i.

$P_{L,i}^{base}$ = real power drawn by load at bus i at the base case operating point.

A higher value of QLI represents higher distance of base case operating point from the maximum loadability point as bus voltages is high. Thus, *QLI* is an index helpful in assessing voltage stability margin (The distance between the base case operating point and maximum loadability point). *QLI* may be enhanced by optimal DG placement/network reconfiguration. Modified QLI after DG placement/network reconfiguration is given by:

$$QLI^m = \sum_{i=1}^{nb} V_i^{REC/DG} P_{L,i}^{base} \tag{38}$$

where, QLI^m = modified network reconfiguration/DG placement.

$V_i^{REC/DG}$ = Voltage at bus i after network reconfiguration/ DG placement. It is apparent that by improving *QLI* by network reconfiguration and DG placement, voltage stability of radial distribution system may be enhanced.

5) ACTIVE POWER LOSS REDUCTION (%*APLR*)

APLR represents percent reduction in active power loss and is given by:

$$\%APLR = (\frac{APL_{old} - APL_{new}}{APL_{old}})100 \tag{39}$$

where, APL_{old} = active power loss in the radial distribution system without DG and/ or reconfiguration.

APL_{new} = active power loss in the radial distribution system with DG and/ or reconfiguration.

6) REACTIVE POWER LOSS REDUCTION (%*QPLR*)

QPLR represents percent reduction in reactive power loss and is given by:

$$\%QPLR = \left(\frac{QPL_{old} - QPL_{new}}{QPL_{old}}\right)100 \tag{40}$$

where, QPL_{old} = reactive power loss in the radial distribution system without DG and/ or reconfiguration
QPL_{new} = reactive power loss in the radial distribution system with DG and/ or reconfiguration

All the indices defined in this section have been summarized in Table 5.

TABLE 5. Performance indices [9] used in this work.

$\%APLR = \left(\frac{APL_{old}-APL_{new}}{APL_{old}}\right) \times 100$
$\%QPLR = \left(\frac{QPL_{old}-QPL_{new}}{QPL_{old}}\right) \times 100$
$NVVB = length(V_i^{REC/DG} < V_{L,min} \text{ and } V_i^{REC/DG} > V_{L,max})$
$VDI = \sqrt{\frac{(\sum_{i=1}^{NVVB}(V_i - V_{limit})^2)}{nb}}\, pu$
$VPI = \sqrt{(\sum_{i=1}^{nb}(V_i^{base} - V_i^{REC/DG})^2)}pu$
$QLI = \sum_{i=1}^{nb} V_i.P_{L,i}^{base}\, pu$
$QLI^m = \sum_{i=1}^{nb} V_i^{REC/DG}.P_{L,i}^{base}\, pu$

VIII. RESULTS AND DISCUSSION

Numerical simulation is accomplished on IEEE 33-bus, 37 branch distribution system [43]. It has 33 buses, 32 generally closed branches and 5 tie switches generally kept open with 3 laterals. The total load demand on substation bus of this RDS constitutes 3.715 MW of real and 3.715 MVAr reactive power. The simulation study is performed using code developed on MATLAB on a system having Intel(R) Core(TM) i7-8700 CPU @ 3.20 GHz processor.

A. WITHOUT CONSIDERING PQV AND P BUSES

Table 6, displays the optimal load flow outcome of IEEE 33-bus distribution system for the different cases under study. It can be realized that only considering PQ buses, 202.68 kW of real power losses incurred in the system at base case. The maximum loadability of the base case system without reconfiguration is found to be 2.63. The farthest bus 18 possesses the lowest voltage of 0.9131 pu in the system.

Table 6, also presents the outcome of reconfiguration with and without DG allocation of the IEEE 33-bus RDS without considering PQV and P buses.

The paper reveals the efficacy of the proposed method to enhance/improve the maximum loadability by simultaneously allocating the DG and reconfiguring the RDS. The system performance enhancements are realized based on the performance indices defined in Table 5. The different results and their comparison with the work in existing literature are accessible in Table 6, Table 7 and Table 8. The consequences of results are analyzed as below:

TABLE 6. Results before P and PQV bus consideration.

Items	Proposed approach*		
	Case 1	Case 2	Case 3
Open Switches	33, 34, 35, 36, 37	7, 10, 14, 28, 32	14, 20, 32, 35, 37
DG MW @bus	—	—	3.6397 @6
APL, (kW)	202.68	140.7058	114.72
QPL (kVAr)	135.14	105.4183	83.799
λ_{max}	2.63	4.26	5.29
NVVB	21	8	0
VDI	0.020197	0.002524	0
VPI	0	0.023689	0.057445
QLI/QLI^m	3.53112	3.579628	3.6527
APLR%	—	30.5764	43.395
QPLR%	—	21.994	37.991
V_{min} @bus	0.9131 @18	0.9413 @32	0.96887 @32
V_{max} @bus	1 @1	1 @1	1 @1

* multi-objective approach as per flowchart in Figure 5

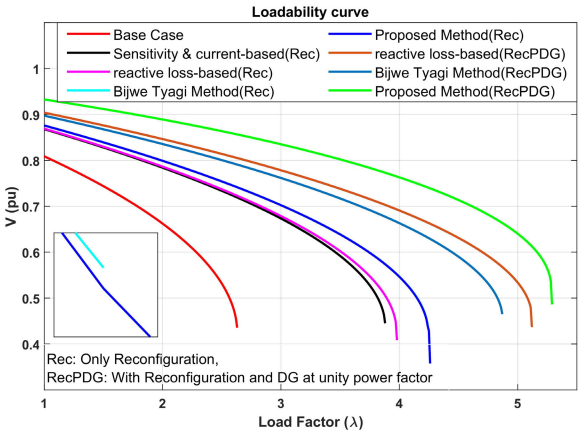

FIGURE 8. Loadability curve for different cases without PQV and P buses.

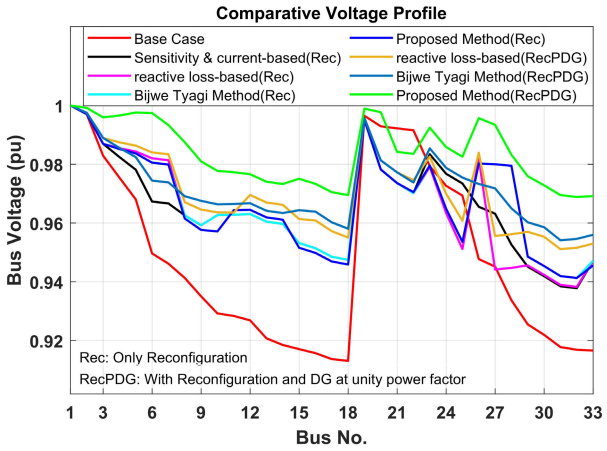

FIGURE 9. Voltage profile for different cases without PQV and P buses.

i. From Table 6, it is perceived that with decrease in APL and QPL enhancement in λ_{max} is observed with reconfiguration and simultaneous application of reconfiguration and DG allocation. The extreme

improvement in λ_{max} is witnessed as 101.14% for Case 3. The Reductions of 30.58% and 21.99% in APL and QPL are noticed, w.r.t. base case. While improvement in the lowest system voltage is achieved to 0.96887 p.u with this case.

ii. The QLI of Case 3 is found to be maximum. With respect to Case 2 the enhancement in QLI for Case 3 is found to be 2.041%.

iii. A noteworthy enhancement in the maximum loadability corresponding to Case 3 has been observed with $\lambda_{max} = 5.29$.

iv. The simultaneous application of optimal DG allocation and reconfiguration enhances the maximum loadability of the RDS without violating the bus voltage limits.

v. From Table 7, It can be noticed that proposed algorithms give the marginally better result than [27] and much better result than [44] and [45] in terms of enhancing the maximum system loadability for Case 2 considering reconfiguration only.

vi. Figure 9 presents the voltage profile of the RDS for cases under study. From Table 6 it is noticed that there are 21 and 8 buses in the RDS which violates the permissible voltage limits for Case 1 and Case 2, respectively. Nevertheless, Case 3 implies a significant enhancement in the RDS voltage magnitude with all the buses voltage lying within the permissible voltage limit.

vii. With the application of reconfiguration and DG injection it is found that Case 3 gives much better results than [27] in terms of maximum loadability as shown in Table 8. Voltage at all the buses lie within the permissible limits.

TABLE 7. Comparison of results for reconfiguration (case 2).

Method	λ_{max}	V_{min}	APL (kW)	Open Switches
Without reconfiguration	2.63	0.9131	202.68	33, 34, 35, 36, 37
Sensitivity approach [44]	3.87	0.9378	139.55	7, 9, 14, 32, 37
current-based approach [45]	3.87	0.9378	139.55	7, 9, 14, 32, 37
reactive loss approach [27]	3.96	0.9383	147.25	7, 9, 14, 26, 32
Bijwe, Tyagi method [27]	4.23	0.9413	139.98	7, 9, 14, 28, 32
Proposed approach	**4.26**	0.9413	140.75	7, 10, 14, 28, 32

B. CONSIDERING PQV AND P BUSES

The efficacy of the method proposed is explained with IEEE 33-bus RDS and associated data are available in [43]. As the primary objective in the presented work is to enhance the maximum loadability of the RDS and to lower the active losses, hence, a suitable designation of 'P' bus should be accomplished.

TABLE 8. Comparison of results for reconfiguration and DG (case 3).

Method	λ_{max}	V_{min}	APL (kW)	Open Switches	DG size @ bus
reactive loss approach [27]	4.86	0.9511	99.77	7, 11, 14, 26, 30	0.25 @ 16, 0.25 @ 17, 0.25 @ 18
Bijwe, Tyagi method [27]	5.11	0.9541	92.91	7, 9, 14, 30, 37	0.25 @ 16, 0.25 @ 17, 0.25 @ 18
Proposed approach	5.29	0.96887	114.72	14, 20, 32, 35, 37	3.6397 @ 6

1) DESIGNATION OF PQV AND P BUSES

For the 33 bus RDS, farthest away bus from substation, having the minimal voltage magnitude in the network as well as the least voltage stability index is designated as PQV bus. In the IEEE 33-bus RDS the farthest away bus is 18^{th} bus on main feeder with voltage magnitude equal to 0.9131 pu. So, to improve the voltage magnitude of this bus, we firstly have chosen this bus as PQV bus with constant voltage of 0.93 pu. To designate a P bus, the main feeder, occupying bus-18 (farthest bus) is chosen. Each and every bus on main feeder (2^{nd} to 17^{th}) are verified to designate P bus for the maximum voltage stability, maximum loadability, and least active power loss.

Table 9 shows the maximum loadability, minimum voltage stability indices, as well as real losses of the RDS to maintain fixed magnitude of voltage at PQV bus corresponding to different sizes of shunt capacitor injecting reactive power at all buses on main feeder. In Table 9, verify that designating 6^{th} bus as P bus, offers the higher maximum loadability, higher voltage stability index, and lowest real power loss for the RDS. Except 6^{th} bus, the characteristics for the P bus selection criterion worsen drastically for other buses when they are designated as P type bus, as shown in Table 9.

Consequently, bus-6 of IEEE 33-bus RDS is designated as the P bus. With load flow of system consisting of PQV and P pair of buses, establishes that shunt capacitor injection of value 1.75353 MVAr at 6^{th} bus leads to enhanced maximum system loadability, highest minimum voltage stability index, and least real power loss of 3.78, 0.7580 pu, and 154.44 kW respectively.

Table 9 clearly depicts that the reactive power required by the shunt capacitor to keep the PQV bus voltage constant at desired set value is lesser when the bus P remains near the PQV bus, though at the cost of higher real power loss and lower loadability and lower voltage stability index. Hence in this work, bus- 6 has been selected as a P bus as it gives better system performance in terms of maximum system loadability, improved voltage stability index, and reduced real power losses.

Table 10 demonstrates the active power loss, loadability, maximum and minimum voltage of the test system before and after the selection of PQV and P bus in the 33 bus system.

TABLE 9. P bus selection criterion.

P bus designated	Shunt Capacitor Injection (MVAr)	λ_{max}	VSI_{min}	APL (kW)
2	54.71986	2.74	0.75206	1727.1
3	8.48739	2.75	0.75214	322.0614
4	5.18178	2.76	0.75211	233.6219
5	3.66845	2.77	0.75212	194.3646
6	**1.75353**	**2.78**	**0.7580**	**154.44**
7	1.21536	2.75	0.74346	159.3741
8	1.09045	2.75	0.73947	162.9015
9	0.82219	2.74	0.7311	168.8629
10	0.659	2.73	0.72612	172.6
11	0.6478	2.73	0.72577	172.93
12	0.6274	2.73	0.72515	173.6
13	0.4846	2.72	0.72084	177.56
14	0.4248	2.72	0.71905	179.39
15	0.390	2.71	0.71799	180.86
16	0.3595	2.71	0.71705	182.29
17	0.2881	2.69	0.71489	185.37

TABLE 10. Results of 33 bus RDS before and after selection of PQV and P buses.

Items	Results of load flow for base case	
	without PQV and P buses	with PQV and P buses
APL (kW)	202.68	154.44
λ_{max}	2.63	2.78
Voltage @bus	V_{min} = 0.9131 @ 18 V_{max} = 1.0 @ 1	V_{min} = 0.93 @ 18 V_{max} = 1.0 @ 1

2) RESULTS FOR VARIOUS CASES CONSIDERING PQV AND P BUSES

Table 11 demonstrates the outcomes of the IEEE 33-bus RDS for the various cases studied with incorporation of the PQV and P buses by proposed algorithm. Some key points of the results are discussed as below:

i. From Table 11 for Case 6, it is perceived that λ increases while APL and QPL decreases reconfiguration and simultaneous application of reconfiguration and DG allocation. The maximum enhancement in λ_{max} is found to be 112.54% for Case 6 (w.r.t. Case 1). The Reductions of 60.857% and 58.947% in APL and QPL are noticed, with respect to base case. The improvement at minimum voltage of the system is achieved as 0.98495 p.u with Case 6.

ii. The maximum value of QLI takes place in Case 6 when DG is placed simultaneously with network reconfiguration optimally. The maximum enhancement in QLI is 3.1727% with simultaneously optimal DG allocation and reconfiguration considering PQV and P buses (w.r.t. Case 1).

iii. A noteworthy enhancement in the VDI is witnessed. The VDI is reduced to zero whereas the index VPI is improved to 0.098197 for Case 6 from zero.

iv. From Table 11, It is noticed that Case 5 does not converge for any solution within the voltage limit. Hence, the lower limit on voltage magnitude is diluted further for convergence.

TABLE 11. Results after P and PQV bus consideration.

Items	Proposed approach*		
	Case 4	Case 5	Case 6
Open Switches	33, 34, 35, 36, 37	7, 9, 14, 32, 37	14, 20, 32, 35, 37
DG MW @bus	—-	——	3.651093 @6
APL, (kW)	154.44	118.1478	69.2
QPL (kVAr)	105.16	89.854	55.48
λ_{max}	2.78	4.08	5.59
NVVB	14	3	0
VDI	0.009141	0.000546	0
VPI	0.005968	0.027159	0.098197
QLI/QLI^m	3.5703	3.6073	3.6932
APLR%	23.801	41.706	65.857
QPLR%	22.184	33.511	58.947
V_{min} @bus	0.9300 @18	0.94772 @33	0.98495 @32
V_{max} @bus	1 @1	1 @1	1.013 @6

* multi-objective approach as per flowchart in Figure 5

v. Figure 11, presents the voltage profile of RDS for cases under study. From Table 11 it is noticed that Case 4 and 5 experiences voltage constraint violation at 14 and 3 number of buses in RDS, respectively while Case 6 ensures there is no voltage limit violation witnessed.

vi. The simultaneous reconfiguration with DG enhances the maximum system loadability of the RDS without voltage limit violation. It is witnessed that proposed algorithm with PQV and P buses provides much better results in terms of maximum loadability, VPI, VDI, NVVB, QLI, APL and QPL of the system.

vii. For Case 6, Table 11 ensures that with proposed multi-objective approach optimal allocation of DG and reconfiguration results in substantial enhancements in Maximum loadability (λ = 5.59), QLI (3.774452), and VPI (0.098197) while the real and reactive losses dropped by 65.857 and 58.947%, respectively.

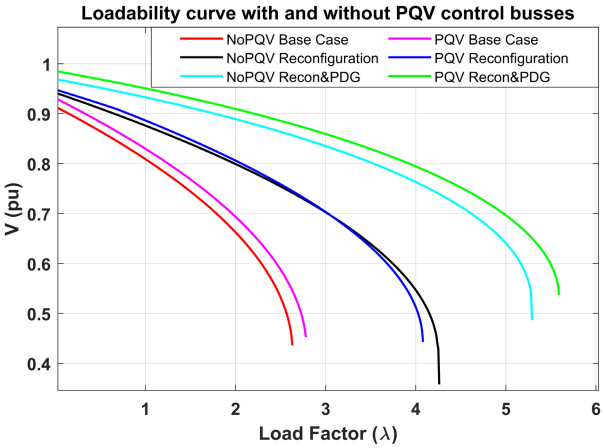

FIGURE 10. Loadability curve for different cases with PQV and P buses.

Consequently, Case 6 awards a considerable enhancement in the performance indices and harvests best maximum

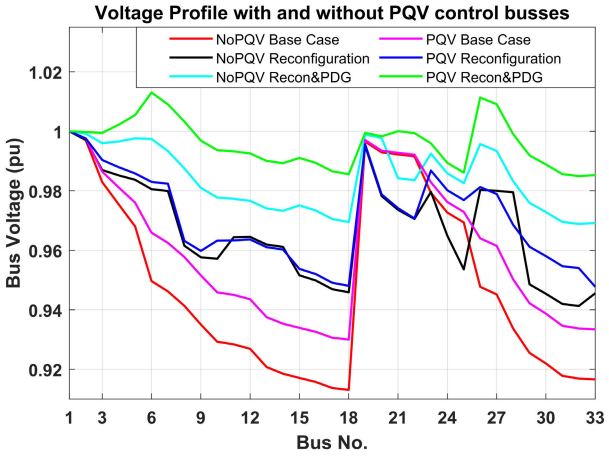

FIGURE 11. Voltage profile for different cases with PQV and P buses.

loadability. The proposed multi-objective algorithm for enhancement of maximum system loadability increases the network loadability with reduction in active power, with all buses within the specified voltage limits.

IX. CONCLUSION

This paper proposes the computational challenges of network reconfiguration problem for enhancement of loadability in distribution system with the simultaneous Distributed generation allocation. Multi-objective meta-heuristic method is used to simultaneously obtain the objectives of loss minimization and voltage stability enhancement. The method uses GWO optimization algorithm to attain the aforesaid objective for loadability enhancement both without and with novel set of PQV and P buses to enhance the loadability of the system and reduce active power losses.

APPENDIX

Simulation Parameters		
DG Rating = 4 MW	Population size = 50	Maximum iterations = 100

REFERENCES

[1] P. Kundur, J. Paserba, V. Ajjarapu, G. Andersson, A. Bose, C. Canizares, N. Hatziargyriou, D. Hill, A. Stankovic, C. Taylor, T. Van Cutsem, and V. Vittal, "Definition and classification of power system stability IEEE/CIGRE joint task force on stability terms and definitions," *IEEE Trans. Power Syst.*, vol. 19, no. 3, pp. 1387–1401, May 2004.

[2] M. M. Mostafa, M. A. Elshahed, and M. M. Elmarsfawy, "Power flow study and voltage stability analysis for radial system with distributed generation," *Int. J. Comput. Appl.*, vol. 137, no. 9, pp. 19–26, Mar. 2016.

[3] V. Ajjarapu and C. Christy, "The continuation power flow: A tool for steady state voltage stability analysis," *IEEE Trans. Power Syst.*, vol. 7, no. 1, pp. 416–423, Feb. 1992.

[4] W. D. Rosehart and C. A. Cañizares, "Bifurcation analysis of various power system models," *Int. J. Electr. Power Energy Syst.*, vol. 21, no. 3, pp. 171–182, Mar. 1999.

[5] M. M. Aman, G. B. Jasmon, A. H. A. Bakar, and H. Mokhlis, "A new approach for optimum simultaneous multi-DG distributed generation units placement and sizing based on maximization of system loadability using HPSO (hybrid particle swarm optimization) algorithm," *Energy*, vol. 66, no. 4, pp. 202–215, 2014.

[6] X. Dou, S. Zhang, L. Chang, Z. Wu, W. Gu, M. Hu, and X. Yuan, "An improved CPF for static stability analysis of distribution systems with high DG penetration," *Int. J. Electr. Power Energy Syst.*, vol. 86, pp. 177–188, Mar. 2017.

[7] N. Mithulananthan and T. Oo, "Distributed generator placement to maximize the loadability of a distribution system," *Int. J. Electr. Eng. Educ.*, vol. 43, no. 2, pp. 107–118, Apr. 2006.

[8] N. C. Hien, N. Mithulananthan, and R. C. Bansal, "Location and sizing of distributed generation units for loadabilty enhancement in primary feeder," *IEEE Syst. J.*, vol. 7, no. 4, pp. 797–806, Dec. 2013.

[9] I. A. Quadri, S. Bhowmick, and D. Joshi, "Multi-objective approach to maximise loadability of distribution networks by simultaneous reconfiguration and allocation of distributed energy resources," *IET Gener., Transmiss. Distrib.*, vol. 12, no. 21, pp. 5700–5712, Nov. 2018.

[10] R. S. Al Abri, E. F. El-Saadany, and Y. M. Atwa, "Optimal placement and sizing method to improve the voltage stability margin in a distribution system using distributed generation," *IEEE Trans. Power Syst.*, vol. 28, no. 1, pp. 326–334, Feb. 2013.

[11] D. Q. Hung and N. Mithulananthan, "Loss reduction and loadability enhancement with DG: A dual-index analytical approach," *Appl. Energy*, vol. 115, pp. 233–241, Feb. 2014.

[12] V. V. S. N. Murty and A. Kumar, "Optimal placement of DG in radial distribution systems based on new voltage stability index under load growth," *Int. J. Elect. Power Energy Syst.*, vol. 69, pp. 246–256, Jul. 2015.

[13] K. Gnanambal and C. K. Babulal, "Maximum loadability limit of power system using hybrid differential evolution with particle swarm optimization," *Int. J. Electr. Power Energy Syst.*, vol. 43, no. 1, pp. 150–155, Dec. 2012.

[14] M. M. Aman, G. B. Jasmon, H. Mokhlis, and A. H. A. Bakar, "Optimal placement and sizing of a DG based on a new power stability index and line losses," *Int. J. Electr. Power Energy Syst.*, vol. 43, no. 1, pp. 1296–1304, Dec. 2012.

[15] P. Karimyan, G. B. Gharehpetian, M. Abedi, and A. Gavili, "Long term scheduling for optimal allocation and sizing of DG unit considering load variations and DG type," *Int. J. Elect. Power Energy Syst.*, vol. 54, pp. 277–287, Jan. 2014.

[16] B. Poornazaryan, P. Karimyan, G. B. Gharehpetian, and M. Abedi, "Optimal allocation and sizing of DG units considering voltage stability, losses and load variations," *Int. J. Elect. Power Energy Syst.*, vol. 79, pp. 42–52, Jul. 2016.

[17] P. Raja, M. P. Selvan, and N. Kumaresan, "Enhancement of voltage stability margin in radial distribution system with squirrel cage induction generator based distributed generators," *IET Gener., Transmiss. Distrib.*, vol. 7, no. 8, pp. 898–906, 2013.

[18] M. A. Kashem, V. Ganapathy, and G. B. Jasmon, "Network reconfiguration for enhancement of voltage stability in distribution networks," *IEE Proc. Gener., Transmiss. Distrib.*, vol. 147, no. 3, pp. 171–175, May 2000.

[19] S. Sivanagaraju, N. Visali, V. Sankar, and T. Ramana, "Enhancing voltage stability of radial distribution systems by network reconfiguration," *Electr. Power Compon. Syst.*, vol. 33, no. 5, pp. 539–550, Mar. 2005.

[20] A. Zidan and E. F. El-Saadany, "Effect of network configuration on maximum loadability and maximum allowable DG penetration in distribution systems," in *Proc. IEEE Electr. Power Energy Conf. (EPEC)*, Aug. 2013, pp. 1–6.

[21] M. H. Hemmatpour, M. Mohammadian, and A. A. Gharaveisi, "Optimum islanded microgrid reconfiguration based on maximization of system loadability and minimization of power losses," *Int. J. Electr. Power Energy Syst.*, vol. 78, pp. 343–355, Jun. 2016.

[22] B. Venkatesh, R. Ranjan, and H. B. Gooi, "Optimal reconfiguration of radial distribution systems to maximize loadability," *IEEE Trans. Power Syst.*, vol. 19, no. 1, pp. 260–266, Feb. 2004.

[23] M. H. Hemmatpour, M. Mohammadian, and A. Gharaveisi, "Simple and efficient method for steady-state voltage stability analysis of islanded microgrids with considering wind turbine generation and frequency deviation," *IET Gener., Transmiss. Distrib.*, vol. 10, no. 7, pp. 1691–1702, May 2016.

[24] N. C. Sahoo and K. Prasad, "A fuzzy genetic approach for network reconfiguration to enhance voltage stability in radial distribution systems," *Energy Convers. Manage.*, vol. 47, nos. 18–19, pp. 3288–3306, Nov. 2006.

[25] M. M. Aman, G. B. Jasmon, A. H. A. Bakar, and H. Mokhlis, "Optimum network reconfiguration based on maximization of system loadability using continuation power flow theorem," *Int. J. Electr. Power Energy Syst.*, vol. 54, pp. 123–133, Jan. 2014.

[26] M. M. Aman, G. B. Jasmon, H. Mokhlis, and A. H. A. Bakar, "Optimum tie switches allocation and DG placement based on maximisation of system loadability using discrete artificial bee colony algorithm," *IET Gener., Transmiss. Distrib.*, vol. 10, no. 10, pp. 2277–2284, Jul. 2016.
[27] A. Tyagi, A. Verma, and P. R. Bijwe, "Reconfiguration for loadability limit enhancement of distribution systems," *IET Gener., Transmiss. Distrib.*, vol. 12, no. 1, pp. 88–93, Jan. 2018.
[28] M. H. Hemmatpour, M. Mohammadian, and M. R. Estabragh, "A novel approach for the reconfiguration of distribution systems considering the voltage stability margin," *Turkish J. Electr. Eng. Comput. Sci.*, vol. 21, pp. 679–698, Mar. 2013.
[29] M. H. Hemmatpour, "Optimum interconnected islanded microgrids operation with high levels of renewable energy," *Smart Sci.*, vol. 7, no. 1, pp. 47–58, Jan. 2019.
[30] M. H. Hemmatpour, M. Mohammadian, and M. Rashidinejad, "A novel reconfiguration mixed with distributed generation planning via considering voltage stability margin," *AUT J. Electr. Eng.*, vol. 43, no. 1, pp. 23–34, 2011.
[31] M. H. Hemmatpour and M. Mohammadian, "An evolutionary approach for optimum reconfiguration and distributed generation planning considering variable load pattern based on voltage security margin," *Arabian J. for Sci. Eng.*, vol. 38, no. 12, pp. 3407–3420, Dec. 2013.
[32] S. G. Ghiocel and J. H. Chow, "A power flow method using a new bus type for computing steady-state voltage stability margins," *IEEE Trans. Power Syst.*, vol. 29, no. 2, pp. 958–965, Mar. 2014.
[33] A. M. Variz, V. M. da Costa, J. L. R. Pereira, and N. Martins, "Improved representation of control adjustments into the Newton–Raphson power flow," *Int. J. Electr. Power Energy Syst.*, vol. 25, no. 7, pp. 501–513, Sep. 2003.
[34] P. A. N. Garcia, J. L. R. Pereira, and S. Carneiro, "Voltage control devices models for distribution power flow analysis," *IEEE Trans. Power Syst.*, vol. 16, no. 4, pp. 586–594, Nov. 2001.
[35] J. Zhao, C. Zhou, and G. Chen, "A novel bus-type extended continuation power flow considering remote voltage control," in *Proc. IEEE Power Energy Soc. Gen. Meeting*, Jul. 2013, pp. 1–5.
[36] A. Tah and D. Das, "Novel analytical method for the placement and sizing of distributed generation unit on distribution networks with and without considering P and PQV buses," *Int. J. Electr. Power Energy Syst.*, vol. 78, pp. 401–413, Jun. 2016.
[37] S. Das, D. Das, and A. Patra, "Reconfiguration of distribution networks with optimal placement of distributed generations in the presence of remote voltage controlled bus," *Renew. Sustain. Energy Rev.*, vol. 73, pp. 772–781, Jun. 2017.
[38] J. Shukla, B. Das, and V. Pant, "Consideration of small signal stability in multi-objective DS reconfiguration in the presence of distributed generation," *IET Gener., Transmiss. Distribution*, vol. 11, no. 1, pp. 236–245, Jan. 2017.
[39] A. Y. Abdelaziz, F. M. Mohamed, S. F. Mekhamer, and M. A. L. Badr, "Distribution system reconfiguration using a modified tabu search algorithm," *Electr. Power Syst. Res.*, vol. 80, no. 8, pp. 943–953, 2010.
[40] E. Dolatdar, S. Soleymani, and B. Mozafari, "A new distribution network reconfiguration approach using a tree model," *World Acad. Sci., Eng. Technol.*, vol. 58, pp. 1186–1193, Oct. 2009.
[41] N. Gupta, A. Swarnkar, and K. R. Niazi, "Reconfiguration of distribution systems for real power loss minimization using adaptive particle swarm optimization," *Electr. Power Compon. Syst.*, vol. 39, no. 4, pp. 317–330, Feb. 2011.
[42] S. Mirjalili, S. M. Mirjalili, and A. Lewis, "Grey wolf optimizer," *Adv. Eng. Softw.*, vol. 69, pp. 46–61, Mar. 2014.
[43] M. E. Baran and F. F. Wu, "Network reconfiguration in distribution systems for loss reduction and load balancing," *IEEE Trans. Power Del.*, vol. 4, no. 2, pp. 1401–1407, Apr. 1989.
[44] G. K. V. Raju and P. R. Bijwe, "An efficient algorithm for minimum loss reconfiguration of distribution system based on sensitivity and heuristics," *IEEE Trans. Power Syst.*, vol. 23, no. 3, pp. 1280–1287, Aug. 2008.
[45] G. K. V. Raju and P. R. Bijwe, "Efficient reconfiguration of balanced and unbalanced distribution systems for loss minimisation," *IET Gener., Transmiss. Distrib.*, vol. 2, no. 1, pp. 7–12, Jan. 2008.
[46] A. Onlam, D. Yodphet, R. Chatthaworn, C. Surawanitkun, A. Siritaratiwat, and P. Khunkitti, "Power loss minimization and voltage stability improvement in electrical distribution system via network reconfiguration and distributed generation placement using novel adaptive shuffled frogs leaping algorithm," *Energies*, vol. 12, no. 3, pp. 1–12, 2019.

AKHILESH KUMAR BARNWAL (Graduate Student Member, IEEE) received the B.Tech. degree in electrical engineering from UPTU, Lucknow, in 2009, and the M.Tech. degree in power systems from the National Institute of Technology, Hamirpur, India, in 2016. He is currently pursuing the Ph.D. degree in electrical engineering with the Indian Institute of Technology (Banaras Hindu University), Varanasi, India. His research interests include power system optimization, renewable energy, distribution system energy management, distribution system planning and operation, voltage stability analysis, smart grid, and load forecasting.

LOKESH KUMAR YADAV received the M.Tech. degree in control system from the National Institute of Technology Patna, India, in 2014, and the B.Tech. degree in electrical and electronics engineering from Uttar Pradesh Technical University, Lucknow, India, in 2011. He is currently pursuing the Ph.D. degree in electrical engineering with the Indian Institute of Technology (Banaras Hindu University), Varanasi, India. He is also an Assistant Professor with the Department of Electrical Engineering, Rajkiya Engineering College, Ambedkar Nagar, Uttar Pradesh, India. His research interests include renewable energy integration in radial distribution systems, optimization techniques, and voltage stability analysis of power systems.

MITRESH KUMAR VERMA (Member, IEEE) received the B.Sc. (Eng.) degree in electrical engineering from the Regional Engineering College, Rourkela (presently National Institute of Technology, Rourkela), India, in 1989, the M.Sc. (Eng.) degree in electrical engineering from the Bihar Institute of Technology, Sindri, India, in 1994, and the Ph.D. degree in electrical engineering from the Indian Institute of Technology (IIT), Kanpur, India, in 2005. He is currently working as a Professor with the Electrical Engineering Department, Indian Institute of Technology (BHU), Varanasi, India. His current research interests include voltage stability studies, application of FACTS controllers, power quality, wide area monitoring systems, and smart grid.